

ARTICLE



Solid papillary mesothelial tumor

Andrew Churg¹✉, Nolwenn Le Stang², Sanja Dacic³, Daniel Pissaloux^{4,5}, Hugues Begueret², Peggy Dartigues², Sophie Giusiano-Courcambec², Ruth Sequeiros², Jean-Claude Pairon⁶, Franck Tirode⁵ and Francoise Galateau-Sallé^{1,2,5}

© The Author(s), under exclusive licence to United States & Canadian Academy of Pathology 2021

We report nine examples of a previously undescribed type of peritoneal circumscribed nodular mesothelial tumor characterized by nests or sheets of mesothelial cells with sharp cell borders and extremely bland, sometimes grooved, nuclei. In some cases, nests were separated by fibrous bands. All patients were women, age range 30–72 years (median 52 years). All tumors were incidental findings during surgery and grossly were either solitary nodules or a few small nodules on the peritoneal surface. Referring pathologic diagnoses included diffuse malignant mesothelioma, localized malignant mesothelioma, well-differentiated papillary mesothelioma, and adenomatoid tumor. No tumor showed BAP1 loss by immunohistochemistry nor deletion of *CDKN2A* by FISH. RNA-seq revealed that these tumors clustered together and were distinct from peritoneal diffuse malignant mesotheliomas. Very few mutations or translocations were found, none of them recurrent from tumor to tumor, and no tumor showed an abnormality in any of the genes typically mutated/deleted in diffuse malignant mesothelioma. Array CGH on three cases revealed two with a completely flat profile and one with a small deletion at 3q26–3q28. On follow-up (range 5–60, median 34 months), there were no deaths, no recurrences, and no evidence of metastatic disease nor local spread; one case that initially had scattered nodules on the pelvic peritoneum had the same pattern of nodules at a second look operation 2 years later. We propose the name solid papillary mesothelial tumor for these lesions. These appear to be either benign or very low-grade tumors that need to be separated from malignant mesotheliomas.

Modern Pathology (2022) 35:69–76; <https://doi.org/10.1038/s41379-021-00899-3>

INTRODUCTION

There are a limited number of neoplastic proliferations of mesothelial cells including malignant mesothelioma (“mesothelioma” in the 2021 World Health Organization (WHO) classification), adenomatoid tumor, and well-differentiated papillary mesothelioma (WDPM; “well-differentiated papillary mesothelial tumor” in the 2021 WHO classification)¹.

In general, these entities are morphologically distinct, but some mesothelial proliferations are difficult to classify and, in particular, are difficult to separate from mesotheliomas. We have recently seen in consultation a number of examples of a different type of small nodular peritoneal mesothelial tumor, mostly encountered as an incidental finding, which did not fit any known neoplastic mesothelial process; most of these were referred, because the original pathologist thought they were malignant. We propose the name “solid papillary mesothelial tumor (SPMT)” for these lesions. Here we describe the morphology, genetic signature, and benign behavior of these tumors.

MATERIALS AND METHODS

Case selection

Ethics approval was obtained from the national and local committee, and approval to use biological samples was obtained (numbers DC2008_586, AC-2013-1806, DR-2011-309, and AC 2011) for cases derived from the

MESOPATH file and from the Research Ethics Board of the University of British Columbia.

Cases were derived from the consultation files of two of the authors (F.G.S. and A.C.). The morphology of each tumor was reviewed by F.G.S., A.C., and S.D., and nine cases with the features described in “Results” were included in this study. All cases were confirmed as mesothelial in origin by commonly used immunohistochemical stains (positive mesothelial markers calretinin, CK5/6, WT-1, D2-40, and negative broad spectrum carcinoma stains). Case 6 had biopsies in 2015 and 2017 (case 7), which were both analyzed morphologically and genetically. Molecular abnormalities and clinical course were compared to a selection from a total of 350 surgical biopsies of peritoneal mesotheliomas from the MESOPATH /MESOBANK files (F.G.S.) diagnosed as non-papillary/non-solid epithelioid mesothelioma ($n = 205$), epithelioid mesothelioma with >50% papillary areas ($n = 50$), and epithelioid mesothelioma with predominantly solid component ($n = 95$).

RNA sequencing

Total RNA was extracted from macrodissected formalin-fixed paraffin-embedded tumor sections using the FormaPure RNA kit (Beckman Coulter #C19158, Brea, CA, USA). RNase-free DNase set (Qiagen #AM2222, Courtaboeuf, France) was used to remove DNA and RNA quantification was assessed using a NanoDrop 2000 (Thermo Fisher Scientific, Waltham, MA, USA). One-hundred nanograms of total RNA were used to prepare libraries with TruSeq RNA UD indexes (Illumina #20022371, San Diego, USA) and TruSeq RNA Exome (Illumina #20020183, San Diego, USA). Twenty-four libraries were pooled at a final concentration of 1.5 nM together with 1% PhiX. Sequencing was performed (paired end, 2 × 75

¹Department of Pathology, Vancouver General Hospital and University of British Columbia, Vancouver, BC, Canada. ²Department of BioPathology Centre Léon Bérard, MESOPATH College, MESONAT, MESOBANK, Lyon, France. ³Department of Pathology, University of Pittsburgh Medical Center, Pittsburgh, PA, USA. ⁴Department of Biopathology, Unit of Molecular Pathology and Cancer Research Center of Lyon, INSERM, Lyon, France. ⁵Team Genetics, Epigenetics and Biology of Sarcomas, Univ Lyon, Université Claude Bernard Lyon 1, INSERM, Cancer Research Center of Lyon, Centre Léon Bérard, Lyon, France. ⁶Faculté de médecine and CHI Creteil, Service de Pathologies professionnelles et de l'Environnement, IST-PE, INSERM, UPEC, Creteil, France. ✉email: achurg@mail.ubc.ca

Received: 20 June 2021 Revised: 6 August 2021 Accepted: 7 August 2021
Published online: 3 September 2021

cycles) with NovaSeq 6000 SP reagent kit (Illumina #20027465) on a NovaSeq 6000 sequencing system (Illumina #20012850).

Alignments were performed using STAR on the GRCh38 version of the human reference genome. Number of duplicate reads were assessed using PICARD tools. No sample was discarded from the analysis (number of unique reads above 10 million). Fusion transcripts were called by five different algorithms, including STAR-Fusion, FusionMap, FusionCatcher, TopHat-Fusion, and EricScript. Expression values were extracted using Kallisto version 0.42.5 tool with GENCODE release 23-genome annotation based on GRCh38 genome reference. Kallisto TPM expression values were transformed in $\log_2(\text{TPM} + 2)$ and all samples were normalized together using the quantile method from the R limma package within R (version 3.1.2) environment. G2M cell cycle score was evaluated by single-sample gene set enrichment analysis (ssGSEA) (<https://github.com/broadinstitute/ssGSEA2.0>) using the HALLMARK_G2M_CHECKPOINT gene set from MSigDB (<https://www.gsea-msigdb.org/gsea/msigdb/>). ssGSEA NES scores were then normalized within an overall series of more than 4500 RNA-sequencing samples, to get a score value ranging from 0 (quiescent cells) to 10 (highly proliferative tumor cells).

Array comparative genomic hybridization

DNA extraction was performed by macro-dissecting formalin-fixed paraffin-embedded tissue block sections followed by the use of the QIAamp DNA micro kit (Qiagen #56304, Hilden, DE). Fragmentation and labeling were done according to the manufacturer's protocol (Agilent Technologies), using 1.5 μg of genomic DNA. Tumor DNA was labeled with Cy5 and a reference DNA (Promega #G1521 or #G1471, Madison, USA) was labeled with Cy3. Labeled samples were then purified using KREApure columns (Agilent Technologies #5190-0418). Labeling efficiency was calculated using a Nanodrop ND2000 Spectrophotometer. Co-hybridization was performed on $4 \times 180\text{K}$ Agilent Sureprint G3 Human oligonucleotide arrays custom (Agilent Technologies #G4125A). Slides were washed, dried, and scanned on the Agilent SureScan microarray scanner. Scanned images were processed using Agilent Feature Extraction software V11.5 and the analysis was carried out using the Agilent Genomic Workbench software.

BAP1 immunohistochemistry

For Vancouver cases, BAP1 immunohistochemistry was run on a Dako Omnis instrument using Santa Cruz antibody C-4 (catalog sc-28383) at 1 : 50 dilution after high pH antigen retrieval. For MESOPATH cases, BAP1 immunostaining were performed on the Benchmark Ultra (Ventana) at the Biopathology department of the Cancer Center Leon Berard, Lyon, using the same antibody from Santa Cruz (C-4) at the same dilution after high pH antigen retrieval.

Fluorescence in situ hybridization

Fluorescence in situ hybridization (FISH) was performed on 4 μm formalin-fixed paraffin-embedded tissue block sections, using the ZytoLight FISH Tissue Implementation Kit (Zytovision #Z-2028-20, Bremerhaven, Germany) and the ZytoLight SPEC CDKN2A locus-specific probe (Zytovision, #Z-2063-200). At least 100 tumor cells were scored by counting the number of copies of *CDKN2A* per nuclei. Homozygous deletion was defined as $\geq 20\%$ of nuclei with a loss of both signals corresponding to *CDKN2A*.

Statistical analysis

Then, χ^2 -test and Fisher's exact bilateral test were used for comparisons between categorical variables and Mann-Whitney test was used for quantitative variables. Univariate analysis was performed for age, sex, and histological subtypes. The survival duration in months was calculated from the date of the initial pathological diagnosis until the date of death or of last follow-up according to Kaplan-Meier methodology. Groups were compared by the log-rank test. Multivariate analysis Cox proportional hazards regression adjusted on age included the factors affecting survival in univariate analysis ($p < 0.20$). Hazard ratios and 95% confidence intervals were computed. Statistical calculations were performed using Stata V13.1.

RESULTS

Clinical and pathologic findings

We studied a cohort of nine cases derived from eight patients. Table 1 shows the demographic and clinical data, and also lists the referring diagnoses. All of the cases were peritoneal lesions in

Table 1. Demographic, clinical, and follow-up data.

Case number	Age/gender	History	Submitting diagnoses	Follow-up
1	30/F	Suspected appendicitis. Appendix normal. Three small nodules discovered on peritoneum, one biopsied	Adenomatoid tumor. Epithelioid mesothelioma	54 Months, NED
2	59/F	6 mm Nodule discovered during treatment for bowel obstruction. History of endometriosis	Well-differentiated papillary mesothelioma	51 Months, NED
3	72F	Follow-up of endometrioid carcinoma—single peritoneal nodule	Epithelioid malignant mesothelioma	41 Months, NED
4	50/F	Focal area of granularity on peritoneum discovered during hysterectomy for adenomyosis	Well-differentiated papillary mesothelioma vs. serous carcinoma	25 Months, NED
5	56/F	Small omental nodule at the time of cholecystectomy. Ovarian tumor 10 years previously	Epithelioid malignant mesothelioma	30 Months, NED
6	35/F	1 cm Nodule on bladder peritoneum at the time of C-section 2015. Multiple tiny nodules on pelvic peritoneum seen but not biopsied	Localized malignant mesothelioma Adenomatoid tumor	See case 7
7	Same patient as no. 6	2017, 20 Small (millimeter) nodules on pelvic peritoneum at laparoscopy for pelvic pain. Nodules grossly unchanged from 2015	Localized malignant mesothelioma	60 Months, no evidence of progressive disease
8	54/F	Incidentally discovered 1 cm nodule at apex vaginal vault/prior hysterectomy	Localized malignant mesothelioma	46 Months NED
9	50/F	Incidentally discovered during a laparoscopy in a patient treated for ductal breast cancer	Diffuse malignant mesothelioma	5 Months, NED

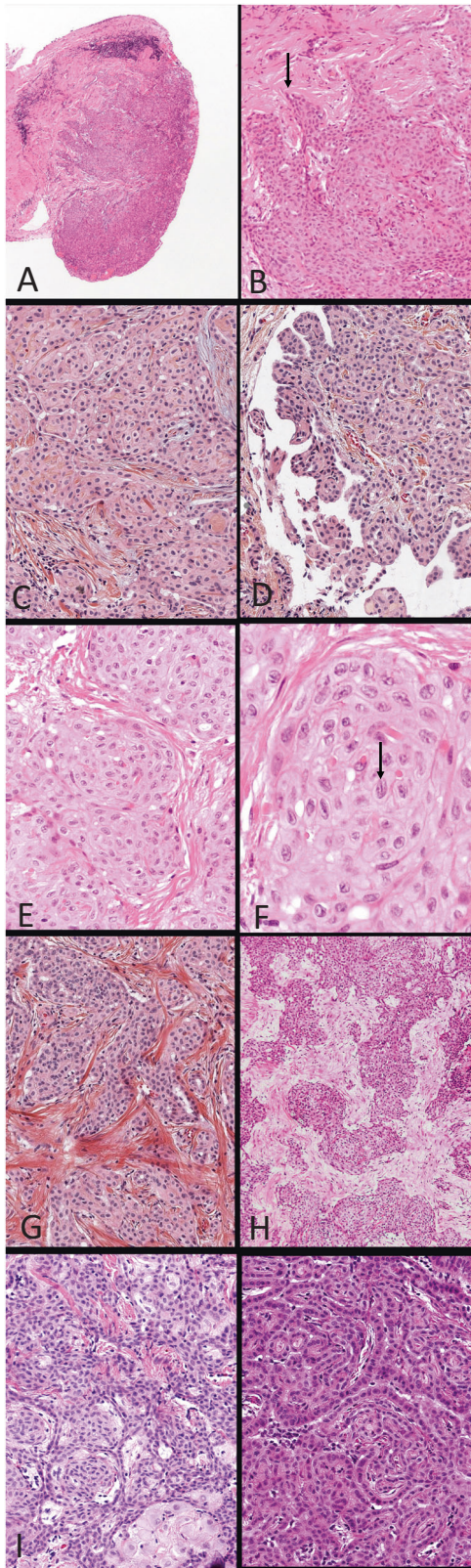


Fig. 1 Microscopic appearances of solid papillary mesothelial tumor (SPMT). **A** Low-power view showing a circumscribed nodule. **B** High-power view of the same nodule showing the irregular interface with the stroma. Pointed nest at arrow suggests invasion, but none of the lesions we report demonstrated tumor cells beyond the circumscribed nodules. **C** Medium power view of a SPMT showing distinct solid tumor nests. **D** Another area of the same tumor shows small papillae. **E** In this example, the tumor nests are separated by fine bands of collagen. **F** Higher-power view of the tumor shown in **E** demonstrates distinct cell membranes. A nucleus with a groove is marked with an arrow. **G** SPMT with distinct fibrous bands separating tumor cell nests. **H** SPMT with nests embedded in an extensive collagenous matrix. **I** SPMT with nests, fine trabeculae of flattened cells, and a few decidual cells at the bottom edge of the field. **J** SPMT with an appearance of collapsed papillae.

multiple (up to 20 nodules) in 4 cases, but no case had diffuse disease mimicking a mesothelioma or metastatic carcinoma. Where information was available, tumor sizes varied from a few millimeters to 1.0 cm.

Figure 1 shows the microscopic appearances of the tumor cells. Tumor cells formed nodules that were circumscribed, but sometimes with an irregular interface with the surrounding stroma (Fig. 1A, B). The tumors were composed of epithelial cells and occasionally slightly spindled cells that marked with typical mesothelial markers. The cells formed sheets or nests (Fig. 1B–I) and in five tumors there were bands of fibrous tissue traversing the tumor (Fig. 1E–H).

In eight of the nine cases, the tumor cells had very distinct sharp cell membranes (Fig. 1C, E, F), although this feature varied from area to area within the tumor. The tumor cell nuclei were always extremely bland, nucleoli were absent or very small, and the nuclei were sometimes grooved (Fig. 1C–G). Necrosis was not present in any case and mitoses were absent to extremely sparse. Overtly papillary structures formed by the same cells were present occasionally as a minor feature (Fig. 1D). In five cases, a minor component of more conventional flattened or cuboidal mesothelial cells forming ribbons or glands (Fig. 1I, J), or areas that looked like compressed papillae (Fig. 1J) were present. In two cases, there was also a minor component of admixed decidual cells (Fig. 1I); these cells were negative for ER α and CD10, and positive for calretinin and WT-1.

Stains for BAP1 were run in all cases and did not show nuclear loss. Similarly, *CDKN2A* FISH did not show homozygous deletion (Table 2). In comparison, BAP1 loss was found in a large fraction (roughly 50%) of the peritoneal mesotheliomas and *CDKN2A* loss by FISH in around 20% (Table 3).

Genetic analysis

Pathogenic mutation and translocation data are presented in Table 2. No pathogenic variants were detected in five cases. In the other four cases, pathogenic somatic variants were few and non-recurrent across the different tumors. Translocations were similarly sparse; none were found in six cases and small numbers were found in the other cases, again with no recurrent translocations across tumors.

Expression profile analyses

Both *t*-distributed stochastic neighbor embedding and hierarchical consensus clustering analyses (Fig. 2A, B), which included a series of epithelioid malignant mesotheliomas with or without solid areas, clearly demonstrated that all SPMT clustered together and away from the mesotheliomas. As shown on Fig. 2B, the SPMT cluster (cluster 6) samples uniformly had a very low G2M cell cycle score.

When looking at immune infiltrate signatures (Fig. 2C), we found that most SPMT samples did not have marked infiltrates

women with a median age of 52 years (range 30–72 years). All except the second look operation (case 7) were incidental findings during surgery for another process. The tumors were generally seen as discrete nodules attached to the peritoneum by a thin pedicle or sessile. Tumors were solitary in 5 cases and were

Table 2. Genomic data.

Case No	RNA-seq: fusion transcripts ^a	Potentially Pathogenic VariantsRNAseq: mutations in Gol ^b	FISH for CDKN2A	aCGH	IHC for BAP1
Case 1	None detected	No variant of interest detected	No deletion of CDKN2A	Flat genomic profile	Retained
Case 2	None detected	TSC2:NM_000548:exon11:c.C11070T;p.A357V IL4R:NM_000418:exon11:c.C1160T;p.S387L	No deletion of CDKN2A	Ish cgh dim(3)(q26.3q28)	Retained
Case 3	IF: FAM195B_ENST00000457257_(e3)--ARHGAP35_ENST00000404338_(e5) F5/NF: MGA_ENST00000219905_(e11)--MFS11_ENST00000586622_(e11) F5/NF: GYS1_ENST00000323798_(e8)--NPLOC4_ENST00000331134_(e13)	MAP3K8:NM_005204:exon4:c.G442A;p.A148T PRKCA:NM_002737:exon9:c.C1010T;p.T337M EP300:NM_001429:exon31:c.A5711C;p.Q1904P	No deletion of CDKN2A	ND	Retained
Case 4	None detected	No variant of interest detected	No deletion of CDKN2A	ND	Retained
Case 5	F5/NF: CEBPB_ENST00000303004_(29pb_inset_e1)--MALAT1_ENST00000610481_(157pb_inset_e2)	No variant of interest detected	No deletion of CDKN2A	ND	Retained
Case 6	None detected	CTNNA1:NM_001903:exon5:c.G503A;p.G168D TNFRSF11A:NM_003839:exon9:c.A1040T;p.D347V	No deletion of CDKN2A	ND	Retained
Case 7 (2ND BIOPSY)	IF: TRAPP10_ENST00000291574_(e21)--FAM207A_ENST00000291634_(e3) F5/NF: CRKL_ENST00000354336_(e2)--SCYL1_ENST00000270176_(e9)	ATM:NM_000051:exon37:c.A5558T;p.D1853V	No deletion of CDKN2A	ND	Retained
Case 8	None detected	No variant of interest detected	No deletion of CDKN2A	Flat genomic profile	Retained
Case 9	None detected	No variant of interest detected	No deletion of CDKN2A	ND	Retained

ND: Not done

^aIF = in frame fusion; F5/NF = frameshift or no frame fusion.^bBenign or likely benign variants are not reported (ClinVar).

Table 3. Comparison of SPMT cases to peritoneal mesothelioma cases.

	EMM* n = 205	Papillary EMM n = 50	Solid EMM n = 95	SPMT n = 9	Comparison test p-Value
Sex					$p < 0.0001^a$
Male	133 (65%)	21 (42%)	60 (63%)	0	
Female	72 (35%)	29 (58%)	35 (37%)	9 (100%)	
Age					$p = 0.0001^a$
Median	66 yrs	62 yrs	70 yrs	50 yrs	
Range	27–90	16–90	39–90	30–71	
CDKN2A deletion	n = 15	n = 5	n = 12	n = 9	$p = 0.58^a$
No deletion	12 (80%)	4 (80%)	10 (83%)	9 (100%)	
Homozygous deletion	3 (20%)	1 (20%)	2 (17%)	0	
BAP1 expression	n = 79	n = 23	n = 47		$p = 0.004^a$
Retained	32 (41%)	13 (57%)	27 (57%)	9 (100%)	
Lost	47 (59%)	10 (43%)	20 (43%)	0	

EMM epithelioid malignant mesothelioma, EMM* epithelial malignant mesothelioma not papillary and not solid, SPMT solid papillary mesothelial tumor.

^ap: χ^2 or Fisher's exact test p-value.

with the exception of two samples containing B- and T-lymphocyte cell populations. As compared with ordinary epithelioid mesotheliomas, SPMT showed less infiltration by lymphocytes. This was also confirmed when we investigated the genes and pathways that are differentially expressed in SPMT compared to epithelioid mesotheliomas (Fig. 2D). Although upregulated genes in SPMT seemed to be involved in cell junctions and vesicular transport, most of the genes under-expressed in SPMT were found to be part of cell cycle/proliferation or immunity pathways.

Array CGH. Array comparative genomic hybridization (CGH) was performed in three cases (Table 2). Two showed a completely flat profile, whereas one showed a heterozygous deletion of 3q26–3q28 (Fig. 3).

Follow-up data

Follow-up data were available for all cases (Table 1) with times ranging from 5 to 60 months (median 43 months). There were no recurrences nor any evidence of development of a malignant mesothelioma. Patient 6 had a second look operation (case 7) 2 years after the initial C-section and the pattern of small pelvic peritoneal nodules was unchanged; this patient is alive and well at 60 months. Supplemental Fig. 1 shows the survival curve for the SPMT cases compared to the 350 epithelioid peritoneal mesotheliomas, tumors that might be viewed as morphologic confounders. Both univariate and multivariate analyses confirmed that SPMT behaves very differently from epithelioid mesotheliomas.

DISCUSSION

In this study, we describe a new type of mesothelial neoplasm that we have labeled SPMT. These tumors have a distinctive morphology with nests and papillae, often compressed, of generally sharply demarcated cells with very bland nuclei and sometimes nuclear grooves. The most important point about these tumors is that they are often mistaken for malignant mesotheliomas, either localized or diffuse (see below), but in fact appear to be either benign or of very low grade.

As indicated in Table 2, SPMT show remarkably few genetic abnormalities and, most importantly, do not show any of the abnormalities recurrently found in malignant mesotheliomas, typically mutation/loss of *BAP1*, *CDKN2A*, *CDKN2B*, *NF2*, *TP53*, *LATS2*, and *SETD2*. Loss of *BAP1* is seen in around 70% of

epithelioid malignant mesotheliomas^{3,4}. Deletion of *CDKN2A* by FISH is seen in some proportion of malignant mesotheliomas, albeit probably less than half of peritoneal epithelioid mesotheliomas⁵ (and Table 3). In contrast, none of our SPMT showed loss of *BAP1* or deletion of *CDKN2A*.

The signaling pathways observed to be dysregulated in this SPMT series were a selection of upregulated genes involved in cell junctions and vesicle transport/microtubules, associated with downregulated genes involving different pathways such as immune response, chemotaxis, calcium homeostasis, proliferation, migration, and blood pressure. The heatmap of immune cells (Fig. 2C) did not highlight a specific immune population in SPMT, with only two tumors having lymphocyte B and T infiltrates, and the others being “cold” with only a few mast cells.

Malignant mesotheliomas commonly show copy number variances, particularly losses. Aneuploidy is extremely common in mesotheliomas, with the majority of tumors showing losses in 1p, 3p, 4, 6q, 9q and 22q, whereas about 25% of mesotheliomas show gains, typically in 17p, 8, 1q, 7p, 15q and 12q². In contrast, two of the three SPMT analyzed by aCGH had flat genomic profiles with no gains or losses; in the third case, there was a small heterozygous deletion in 3q26–3q28. Gene expression cluster analysis showed that these tumors are molecularly distinct from epithelioid malignant mesotheliomas and have very low cell cycle scores, scores at the level of benign tumors.

Although SPMT can have papillary areas, these are typically minor and quite different from the edematous papillae with a covering layer of single bland mesothelial cells that, by definition, characterize WDPMT tumor (WDPMT). SPMT also appear to be genetically distinct from WDPMT, although the latter statement is made with caution, because only two reports have addressed the genetics of WDPMT. Shrestha et al.⁶ reported that five cases of WDPMT had recurrent mutations in *EHD1*, *ATM*, *FBXO10*, *SH2D2A*, *CDH5*, *MAGED1*, and *TP73*, whereas Stevers et al.⁷ analyzed ten cases and found mutations in *TRAF7* and *CDC42*. In 2020, MESOPATH analyzed 30 cases of WDPMT from the peritoneum and observed few mutations in *TRAF7* (4/30; 13%) or *CDC42* (5/30; 17%), and no mutations in WDPMT of the pleura ($n = 4$) (Galateau-Salle et al., unpublished data). Apart from one SPMT with an *ATM* mutation, none of the mutations described in WDPMT were found in SPMT. SPMTs are also different morphologically and genetically from adenomatoid tumors, which typically form simple glands rather than being solid proliferations and are reported to show *TRAF7* mutations^{8,9}.

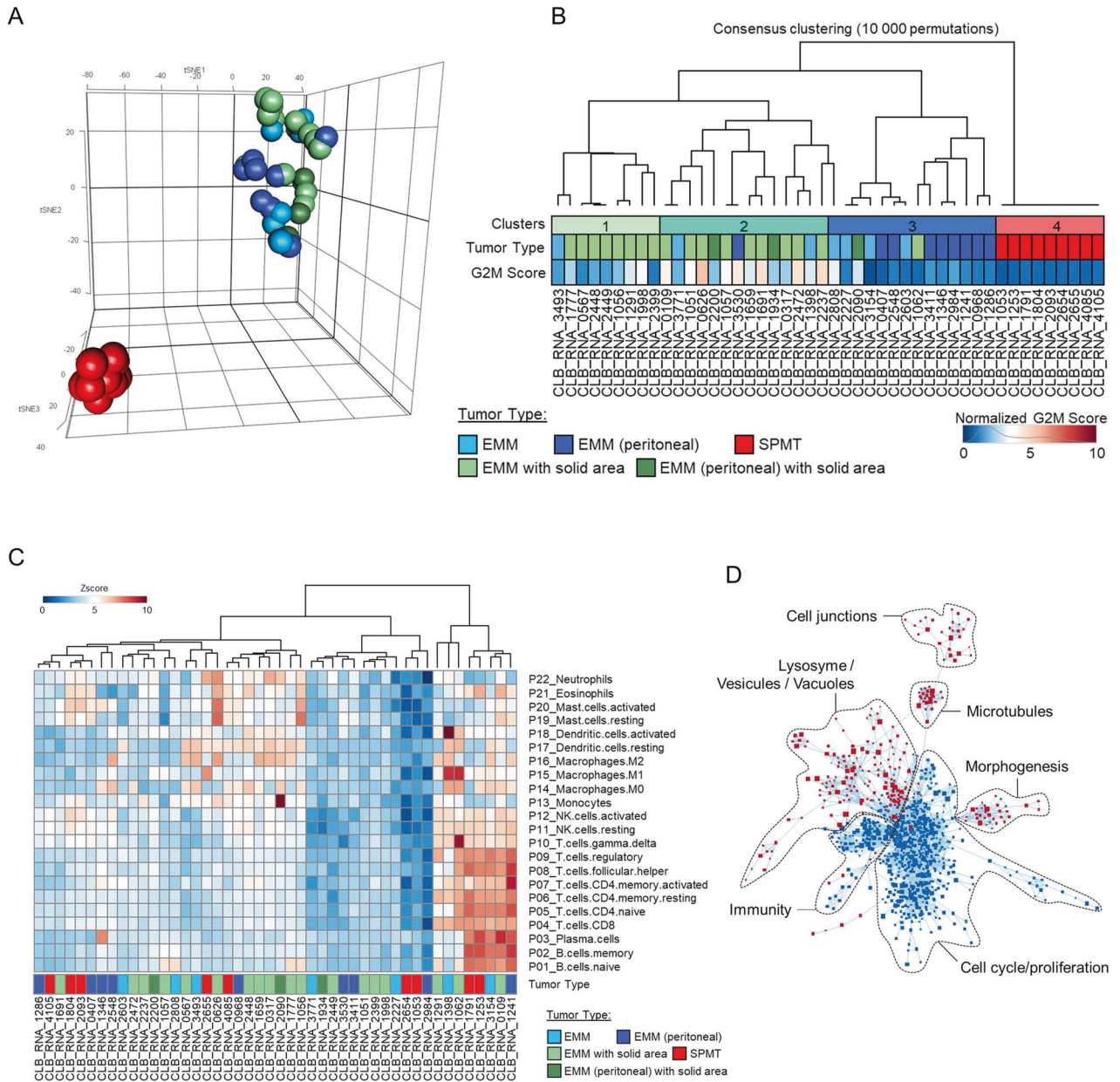


Fig. 2 RNA-sequencing expression profile analyses. **A, B** The *t*-distributed stochastic neighbor embedding (**A**) and hierarchical consensus clustering (**B**) demonstrate that SPMT (in red) are completely separate from the mesotheliomas. **C** Hierarchical consensus clustering based on the ssGSEA NES score for each cellular population of the LM22 signatures. **D** Cytoscape representation of GSEA analysis on differentially expressed genes in SPMT as compared to the other samples highlighting that downregulated genes are mostly involved in cell cycle/proliferation, whereas upregulated ones are related to cell junctions or vesicle transport.

Although the genetics appear to separate these entities, the major morphologic differential diagnosis for SPMT is nonetheless a malignant mesothelioma, either diffuse or localized; indeed, most of these tumors were viewed as diffuse or localized malignant mesotheliomas by the referring pathologists (Table 1). It is noteworthy that in this series SPMT only occurs in women, as opposed to diffuse peritoneal mesotheliomas, which affect both genders and which occur at a later age (Table 3). Diffuse malignant mesotheliomas usually show peritoneal “carcinomatosis,” i.e., widespread nodules or sheets of tumor cells diffusely distributed in the peritoneal cavity, whereas many SPMT are solitary nodules, and even in the cases with more than one tumor nodule, these nodules were confined to a localized area. Malignant mesotheliomas often, but not always, have cytologically

much higher nuclear grade and we have never seen a mesothelioma with nuclear grooves. Mesotheliomas also do not have cells with sharply demarcated cell membranes, except for some cases of transitional mesothelioma. However, the latter are a form of sarcomatous mesothelioma (and sarcomatous mesotheliomas are very rare in the peritoneal cavity) and in our experience are invariably visually of much higher grade¹⁰. Malignant mesotheliomas can have necrosis, a feature not seen in any of SPMT. Mitoses are the rule in malignant mesotheliomas, but seven of our nine SPMT cases did not have any mitoses and the other two had fewer than two per 2 mm². Malignant mesotheliomas, by definition, are infiltrative tumors and invasion of fat or another organ would support a diagnosis of malignancy. SPMT are not infiltrative, although the edges of SPMT can show irregular

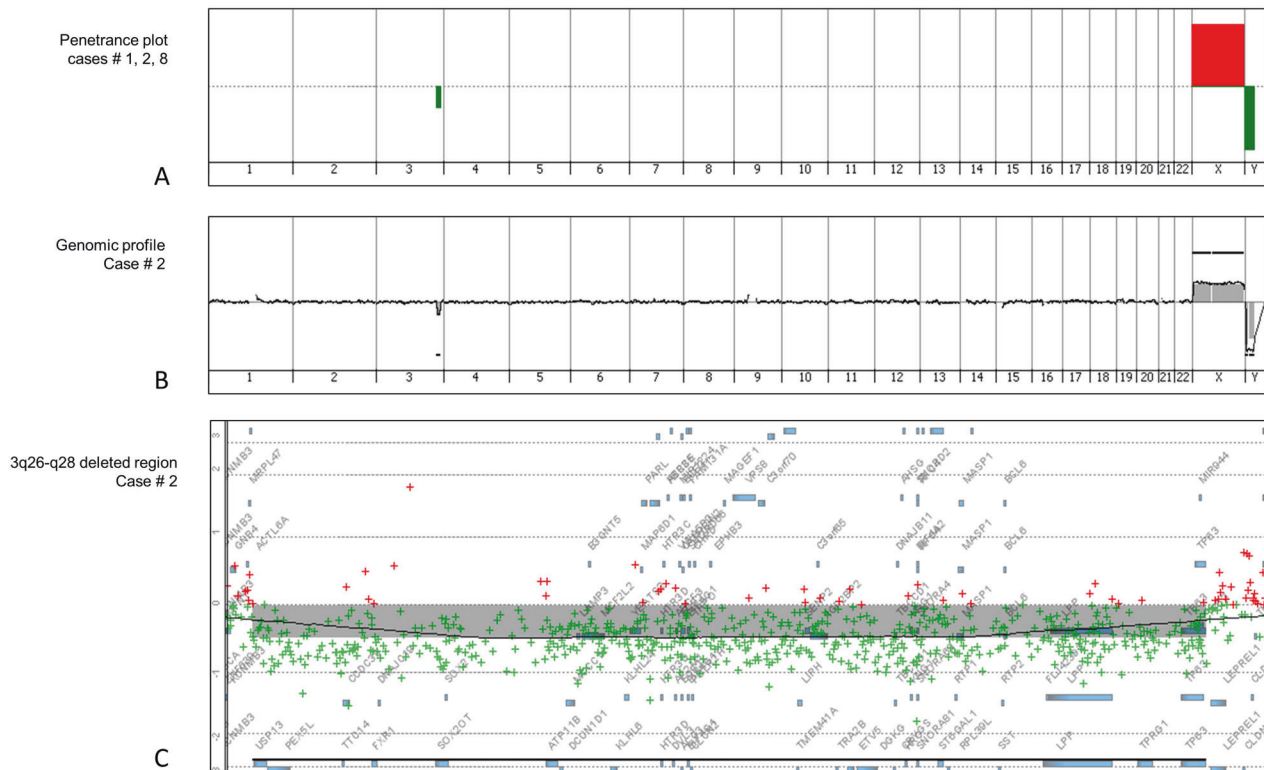


Fig. 3 aCGH data. **A** Penetrance plot for all three cases studied. **B** Case 2, which showed a small deletion at 3q26–3q28. **C** Details of the deleted region in case 2.

extension into the capsule or pseudocapsule, and this could cause confusion with malignant mesotheliomas.

Localized malignant mesotheliomas, which are always solitary nodules, are potentially a more difficult differential diagnosis, but localized malignant mesotheliomas are extremely rare and not well characterized in the peritoneal cavity¹¹. Extrapolating from pleural tumors, localized malignant mesotheliomas microscopically look like diffuse mesotheliomas, so that their cytologic characteristics are similar to those described above for diffuse mesotheliomas. Pleural localized mesotheliomas are genetically similar to pleural diffuse mesotheliomas¹². In the equivocal case with a differential of diffuse or localized mesothelioma, genomic analysis may be necessary to separate these entities; in particular, the finding of mutation/deletion of *MTAP*, *BAP1*, *CDKN2A*, *CDKN2B*, *NF2*, *TP53*, *LATS2*, or *SETD2* by immunohistochemistry, FISH, or sequencing, or significant copy number alterations, favor a diagnosis of malignancy.

Lastly, caution should be exercised when making a diagnosis of SPMT in regards to indicating prognosis. On the basis of a limited number of cases, some with short follow-up times, these tumors appear to be benign and probably can be treated with local excision, but the possibility that they are of very low-grade malignancies cannot be excluded from our data. However, they are clearly different from the much more aggressive diffuse or localized malignant mesotheliomas (Supplemental Fig. 1).

DATA AVAILABILITY

Detailed molecular data are available from the authors

REFERENCES

1. WHO Classification of Tumours Editorial Board. *Thoracic Tumours. WHO Classification of Tumours Series* 5th edn, Vol. 5, <https://publications.iarc.fr/595> (International Agency for Research on Cancer, 2021).

2. Wadowski, B., De Rienzo, A. & Bueno, R. The molecular basis of malignant pleural mesothelioma. *Thorac Surg. Clin.* **30**, 383–393 (2020).
3. Wang, L. M. et al. Diagnostic accuracy of BRCA1-associated protein 1 in malignant mesothelioma: a meta-analysis. *Oncotarget* **8**, 68863–68872 (2017).
4. Leblay, N. et al. BAP1 is altered by copy number loss, mutation, and/or loss of protein expression in more than 70% of malignant peritoneal mesotheliomas. *J. Thorac. Oncol.* **12**, 724–733 (2017).
5. Singhi, A. D. et al. The prognostic significance of BAP1, NF2, and CDKN2A in malignant peritoneal mesothelioma. *Mod. Pathol.* **29**, 14–24 (2016).
6. Shrestha, R. et al. Well-Differentiated papillary mesothelioma of the peritoneum is genetically distinct from malignant mesothelioma. *Cancers (Basel)* **12**, 1568 (2020).
7. Stevers, M. et al. Well-differentiated papillary mesothelioma of the peritoneum is genetically defined by mutually exclusive mutations in TRAF7 and CDC42. *Mod. Pathol.* **32**, 88–99 (2019).
8. Goode, B. et al. Adenomatoid tumors of the male and female genital tract are defined by TRAF7 mutations that drive aberrant NF- κ B pathway activation. *Mod. Pathol.* **31**, 660–673 (2018).
9. Itami, H. et al. TRAF7 mutations and immunohistochemical study of uterine adenomatoid tumor compared with malignant mesothelioma. *Hum. Pathol.* **111**, 59–66 (2021).
10. Galateau-Salle, F. et al. Comprehensive molecular and pathologic evaluation of transitional mesothelioma assisted by deep learning approach: a multi-institutional study of the International Mesothelioma Panel from the MESOPATH Reference Center. *J. Thorac. Oncol.* **15**, 1037–1053 (2020).
11. Marchevsky, A. M. et al. Localized malignant mesothelioma, an unusual and poorly characterized neoplasm of serosal origin: best current evidence from the literature and the International Mesothelioma Panel. *Mod. Pathol.* **33**, 281–296 (2020).
12. Hung, Y. P. et al. Molecular characterization of localized pleural mesothelioma. *Mod. Pathol.* **33**, 271–280 (2020).

ACKNOWLEDGEMENTS

Experts of MESOPATH College: G. Averous, H. Begueret, M. Brevet, A. Cazes, M.C. Copin, D. Damotte, C. Danel, P. Dartigues, J. Fontaine, A. Foulet-Roge, F. Galateau Sallé, L. Garbe, S. Giusiano-Courcambeck, L. Garbe, V. Hofman, S. Humez, S. Isaac, S. Lantuejoul, E. Mery, J.M. Picquenot, N. Piton, G. Plancharde, I. Rouquette, P. Rouvier, C. Sagan, F. Thivolet, S. Valmary-Degano, and J.M. Vignaud. We thank the case

contributors Dr A.Y. Delajarte, Vaquer J.M., Belleannée G., Familiades P., Morcos M., Cohen C., Guillaubey C., De Queiros F., Longchamp E., Marty M., Daubech A., Diebold M.D., and Mansuet Lupo A. We are extremely grateful to the Department of Biopathology and also thank the Human Tissue Resource Center MESOBANK France for materials with S. Tabone; Clara Farge for her expertise in performing WSI and technical assistance in scanning slides; J.P. Michot, S. Paindavoine, F. Dreux, A. Houlier, C. Taillandier, C. Py, and E. Malandain for their great technical assistance in RNA sequencing and immunohistochemistry, and MESOPATH team A. Nguyen Phuong, F. Damiola, E. Pean, and Pr. Jean Yves Blay.

AUTHOR CONTRIBUTIONS

Study design: A.C., F.G.S., S.D., and F.T. Data acquisition and analysis: A.C., F.G.S., S.D., F.T., and N.L.S. Manuscript drafting: A.C., F.G.S., S.D., F.T., N.L.S., D.P., H.B., P.D., S.G.-C., R.S., and J.P.

FUNDING

This work was supported by a French National Cancer Institute core grant and the French Health National Institute Santé Publique France.

COMPETING INTERESTS

The authors declare no competing interests.

ETHICS APPROVAL AND CONSENT TO PARTICIPATE

Ethics approval was obtained from the national and local committee, and approval to use biological samples was obtained (numbers DC2008_586, AC-2013-1806, DR-2011-309, and AC 2011) for cases derived from the MESOPATH file and from the Research Ethics Board of the University of British Columbia.

ADDITIONAL INFORMATION

Supplementary information The online version contains supplementary material available at <https://doi.org/10.1038/s41379-021-00899-3>.

Correspondence and requests for materials should be addressed to Andrew Churg.

Reprints and permission information is available at <http://www.nature.com/reprints>

Publisher's note Springer Nature remains neutral with regard to jurisdictional claims in published maps and institutional affiliations.